Chemometrics and Intelligent Laboratory Systems 97 (2009) 46–51

Contents lists available at ScienceDirect

Chemometrics and Intelligent Laboratory Systems

journal homepage: www.elsevier.com/locate/chemolab

Application of nonlinear PCR for optimization of hybrid binder used in construction materials

I.A. Starovoitova [a], V.G. Khozin [a], L.A. Abdrakhmanova [a], O.Ye. Rodionova [b], A.L. Pomerantsev [b,*]

[a] Kazan State University of Architecture and Engineering, Zelenaya str. 1, Kazan, 420043, Russia
[b] Institute of Chemical Physics RAS, Kosygina str. 4, Moscow, 119991, Russia

ARTICLE INFO

Article history:
Received 29 April 2008
Received in revised form 20 July 2008
Accepted 22 July 2008
Available online 5 August 2008

Keywords:
PCA
Nonlinear PCR
Water glass
Polyisocyanate
Composite material

ABSTRACT

The research is aimed at optimization of a hybrid binder formulation that includes water solution of sodium silicate (water glass) and polyisocyanate. Optimization is performed with respect to ten output quality characteristics. Calibration modeling is done as a two-step procedure. At first, PCA is applied to the **X** block for variable reduction. Then nonlinear regression is used to predict a particular quality characteristic as a function of score vectors. The input variables reduction enables to choose an optimal binder formulation that meets the predefined quality requirements. The prediction has been confirmed by the verification experiments.

1. Introduction

Nowadays chemometrics is a universally recognized tool within analytical chemistry. However, beyond this area the multivariate approach (MVA) is not as widely applicable as it actually deserves. Multivariate statistical process control (MSPC) is the only exception that proves the rule. Even so, the authors believe that MVA could be of a large merit being applied in engineering, in general, and in the optimization of the material formulations, in particular. Recent studies of the latent variables (LV) based optimization performed by J. MacGregor [1,2] and A. Höskuldsson [3,4] have demonstrated a great potential of such an approach. In particular, it has been shown that optimization within the LV space leads either to the border located solutions [3] or to the nonlinear reconstruction of the model [1]. Typically, nonlinear PLS [5,6] serves for such a rebuilding, but nonlinear PCA [7] may be used as well.

All these complicated issues – LV based optimization and nonlinear PCA – are employed in this short communication that presents a simple solution of a highly practicable problem, namely, optimization of a hybrid binder formulation used in civil engineering. In our opinion, the paper has two main merits. At first, it demonstrates implementation of the chemometric approach to a novel area that is civil engineering where such methods are still not widely known. The second merit is, in some sense, a methodological gain. So far, the LV space optimization is a novel, establishing trend in chemometrics. The objects are too complicated, the methods are too sophisticated. Therefore a straightforward example with a clear visually proved LV space optimization could be of interest for the chemometric community.

Binder is the important constituent that has a great influence on the properties of the final composite material. The type of binding determines not only the strength characteristics, but also thermostability, water resistance, insulation, and other properties. At the same time a binder should be simple in treatment, has a low shrinkage volume at hardening, be a non toxic, and has a low cost. Therefore, optimization of the binder composition is of vital importance.

Water glass (WG) is the aqueous solution of sodium silicates and polysilicates. It is a colourless, transparent, glasslike substance that is applied in industry since the end of the 19-th century due to its adhesive properties. WG is used as a binder in composite materials [8], which are further utilized in production of various construction materials. In the building industry the main areas of WG applications are as follows: consolidation and stabilizing of the rock bed and ground; production of porous materials, silicate paints, varnishes, and glues. It is also used in production of the fire- and acid-proofing concretes and the fire-retarded coatings [9].

The WG based materials are simple in production; they are known for their high heat-, acid- and fire-resistance and stability. The shortcomings of the compositions containing WG are the low water resistance, shrinkage in the course of hardening, fragility, and the low dynamic force resistance. Various modifying agents are added to WG to eliminate these shortcomings. The most interesting are the organic additives. Hybrid organic–inorganic compositions form a special class

* Corresponding author.
E-mail address: forecast@chph.ras.ru (A.L. Pomerantsev).

0169-7439/$ – see front matter © 2008 Elsevier B.V. All rights reserved.
doi:10.1016/j.chemolab.2008.07.008

inside the composite materials. There have been the numerous publications [10–14] devoted to synthesis of the hybrid materials based on WG and hydrophilic or hydrophobic oligomers. As a rule, such synthesis is conducted in the presence of some diluents.

Synthesis of the hybrid material with silicates, which are not modified organically, is not so wide spread. It has been reported [15] about the synthesis of organic–inorganic composition on the base of the urethane oligomer and the water solution of sodium silicate. This composition has a high water sorption and thus it may be used as a gel electrolyte, or as a hydrogel in the drug delivery systems. Properties of the hybrid resins have been investigated in [16]. These materials comprise epoxide resins, polyisocyanate, WG, and emulsifying agent. However, these binders have a low water resistance. Moreover a toxic chlorine-containing emulsifying agent, namely, tris-(1-chloro-2-propyl)phosphate, is used in production.

Organic-silicate materials, which are produced from WG and polyisocyanate, have been synthesized and investigated in the Kiev Institute of Macromolecular Chemistry [17,18]. Addition of plasticizing agents and catalysts helps to improve the compression strength up to 30–59 MPa [19]. The shortcoming of these materials is a long curing time that is about 30 days.

Our group in the Kazan State University of Architecture and Engineering has synthesized the hybrid organic–inorganic binders, which have both high strength and water resistance characteristics. They are also thermo stable up to 270–280 °C. Unfortunately the hardening is lasted for 30–45 days at temperature 20–25 °C. The IR spectroscopy shows that isocyanate groups are consumed slowly, and after 20 days of hardening the contents of unreacted isocyanate groups is 20–30% [17]. Such the long curing time is an obstacle for the industrial production. To decrease the processing time a special stepwise heating has been proposed [20]. The first step is continued for 1–1.5 h at temperature 80–85 °C, the second step is conducted for 2–7 h at 95–100 °C. After such a processing the share of the unreacted isocyanate groups is less than 10%.

The object of the presented study is optimization of the hybrid organic–inorganic composition in order to obtain the binder with the desirable properties.

2. Experimental

2.1. Materials and sample preparation

Polyisocyanate (PIC) is a heterocyclic aromatic compound R-$(NCO)_2$ that contains two terminal isocyanate groups having a high degree of unsaturation. PIC is a viscous dark brown liquid with molecular mass about 1000 and density 1.25 g cm^{-3}. The content of reactive NCO groups is 31–32%. Water glass (WG) is aqueous solution of sodium silicates and polysilicates different in the ratio of silicon and sodium oxides and density. Molar ratio SiO_2/Na_2O is one of the basic features of WG.

Binders were obtained by mixing of PIC and WG in the laboratory mixer for 2–3 min. The ratio of the reactive groups NCO:OH was from 1:1 to 1:3. Compositions were preliminary soaked under the normal conditions during 16–20 h. Hardening was performed with the step heating till 100 °C. At this temperature the binder was cured for 2–7 h depending on the formulation.

2.2. Methods of measurements

Several tests were performed with a fresh liquid binder and others with a hardened composite.

Viscosity was measured as the time (s) of the fresh binder (100 ml) outflow from the viscosimeter with the nozzle diameter of 4 mm.

Gelatination is the time (min) between the components mixing and the complete loss of reciprocal viscosity at 20 ± 2 °C.

Wetting angle was estimated as the contact angle between the fresh binder and glass. For this purpose a drop of binder is placed on a glass plate. The scaled microscope is used to determine the height and diameter of the drop with subsequent calculation of wetting angle.

Conversion rate of NCO groups was obtained by IR spectroscopy. The samples of the hardened binders are ground with vibratory mill to a fine powder and mixed with vaseline. IR spectra were acquired through the KBr windows in the range 4000–400 cm^{-1}. Conversion was measured as the signal intensity at wavenumber 2272 cm^{-1}, which is responsible for isocyanate vibration. The signal at range 1568–1623 cm^{-1} was utilized as the «internal standard».

Compression strength and modulus of elasticity in compression were measured with the hardened binder using the cylinder samples of 15 mm in diameter and 24 mm in height. The test is done applying the tearing machine with the loading rate of 10 mm/min. Prior to the testing, the sample height and diameter are measured. Compression strength (kg cm^{-2}) is calculated as $\sigma = P/S$, where P is the breaking stress and S is the cross-section area of the unloaded sample.

Modulus of elasticity E in compression was calculated as the slope of the initial, linear-elastic part of the stress–strain diagram.

Thermal stability was investigated by load-indentation measurement at tempering of the hardened binder. The samples have a tablet form of 3 mm thickness. They were loaded under the stress of 5000 g with a cylinder intender having 1 mm^2 tip area. The heating device provided the constant temperature rate of 50 °C/h. The temperature at which the indenter penetrated into the sample to 1 mm depth is registered as the thermal stability indicator.

Hardness was measured with the ball indenter applied to the hardened binder samples that have a plate form of 5 mm by 15 mm. The 5 mm steel ball was pressed into the sample under the stress of 980 N for 30 s. The hardness is calculated by formula: $H = P/(\pi dh)$, where P is the stress; d is the ball diameter; h is the imprint depth.

Water resistance was investigated by boiling of the hardened binder samples for 3 h. This characteristic is calculated as the relative weight loss: $\Delta m = (1 - m_2/m_1)$, where m_1 is the weight of the sample before boiling, m_2 is the weight of the sample dried after boiling.

2.3. Data set description

The data were obtained at fractional factorial experiment with 27 binder formulations. Each sample was measured three times for every property characteristics. Factors that first and foremost influence on forming of the chemical and phase structure are collected in the input block. They are the SiO_2/Na_2O weight ratio (x_1), WG density (x_2), water contents in WG (x_3), PIC contents (x_4), and WG glass contents (x_5). Other ten material properties are treated as the responses. They can be divided into the processing characteristics, such as processing time (y_1), viscosity (y_2), gelatination time (y_3), limiting wetting angle (y_4), and the final composite properties, such as hardness (y_5), compression strength (y_6), modulus of elasticity in compression (y_7), thermal stability (y_8), water resistance (y_9), and conversion level (y_{10}). The composite properties were studied in a wide quantity range, i.e. the thermal stability varied from 190 °C to 280 °C, the compression strength changed in the range of 40–100 MPa, and hardness varied from 160 kg cm^{-3} to 275 kg cm^{-3}.

2.4. Methods

Three replicas were averaged to obtain the predictor matrix **X** (27×5) and response matrix **Y**(27×10). Matrices **X** and **Y** were the column-wise centered and scaled.

Data analysis is conducted in two steps. At first, PCA is applied to the **X** block for variable reduction, $\mathbf{X} = \mathbf{TP}^{\mathrm{T}} + \mathbf{E}$. Afterwards the multiple regression of **Y** upon **T** is constructed. Namely, each response variable y_j ($j = 1,\ldots,10$) is modeled using a quadratic equation

$$y_j = b_{00}^{(j)} + b_{01}^{(j)} t_1 + b_{02}^{(j)} t_2 + b_{11}^{(j)} t_1^2 + b_{12}^{(j)} t_1 t_2 + b_{22}^{(j)} t_2^2 + e_j, \quad (1)$$

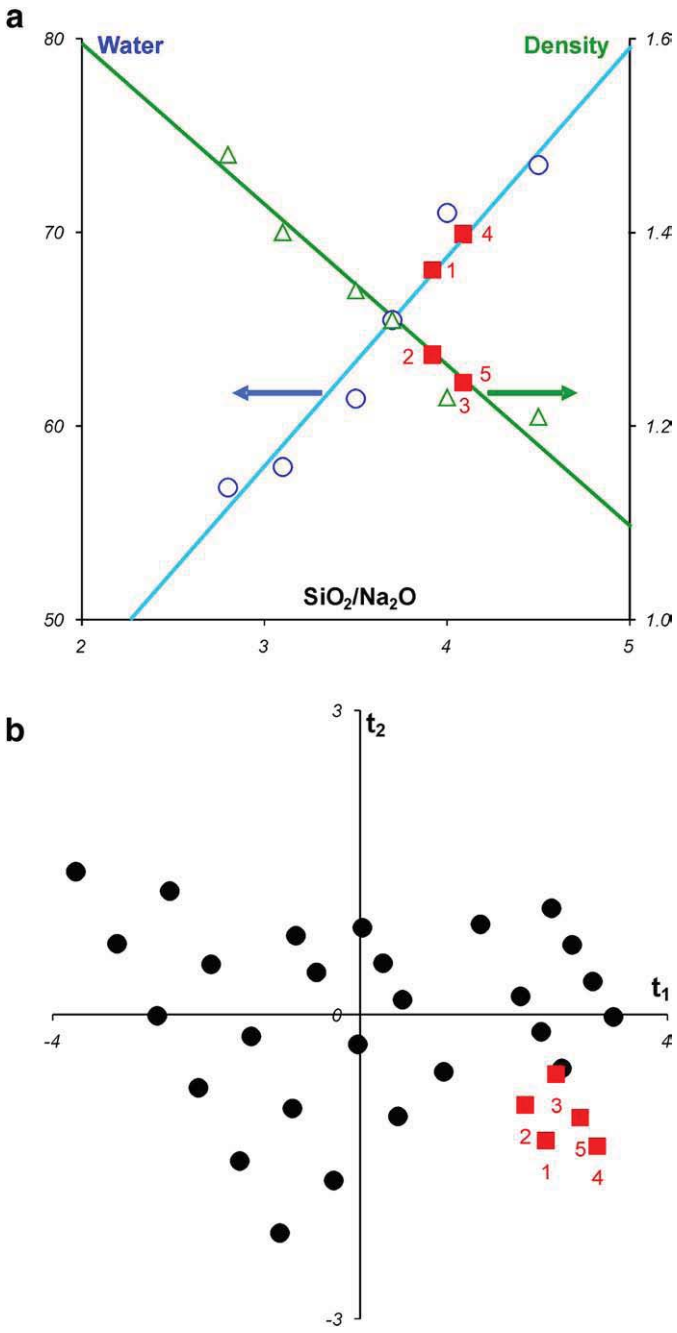

Fig. 1. Experimental *X* data. Squares are the optimized candidates. a) x_1 vs. x_2, left axis; x_1 vs. x_3, right axis, b) Scores plot. Dots are calibration points.

where t_1 and t_2 are elements of the PCA score vectors, and $\boldsymbol{b}_{kl}^{(j)}$ are the regression coefficients. As each score vector $\boldsymbol{t}_i$ is a linear combination of the initial predictor variables $\mathbf{x}$, we obtain a nonlinear regression model that describes a response property subjected to the $\mathbf{X}$ values. The whole two-step procedure could be considered as a nonlinear PCR (NPCR).

These 10 regression models (for $y_1,\ldots, y_{10}$) are utilized for solving optimization problem. Optimized candidate points $\mathbf{t}_{opt} = (t_1^{opt}, t_2^{opt})$ are sought in the score space with a simple visual inspection of all contour maps, which reflect the *y* levels versus PCs (t_1, t_2). Predicted *Y*-values are calculated by Eq. (1) at $\mathbf{t} = \mathbf{t}_{opt}$. The optimal points presented in the original predictor coordinates are found applying equation $\mathbf{x}_{opt} = \mathbf{t}_{opt}\mathbf{P}^T$. Obtained $\mathbf{x}_{opt}$ formulations are employed for making of new samples that participate in the verification experiment.

3. Results and discussion

3.1. Modeling

Studding the initial data set we can mark a strong positive correlation between variables x_1 (SiO_2/Na_2O molar ratio) and x_2 (water contents), and negative correlation between x_1 and x_3 (WG density) (see Fig. 1a).

With increasing of x_1 from 2.8 to 4.5 units, the water content (open dots, left vertical axis) is changing almost linearly from 55 till 75%. At the same time the WG density (open triangles, right vertical axis) is decreasing from 1.48 g cm^{-3} till 1.12 g cm^{-3}. Variable x_4 and x_5 are connected by the following equation $x_4 + x_5 = 100\%$. Thus input variables are not independent and application of the projection methods may result in variable reduction. However, direct application of PLS/PCR for

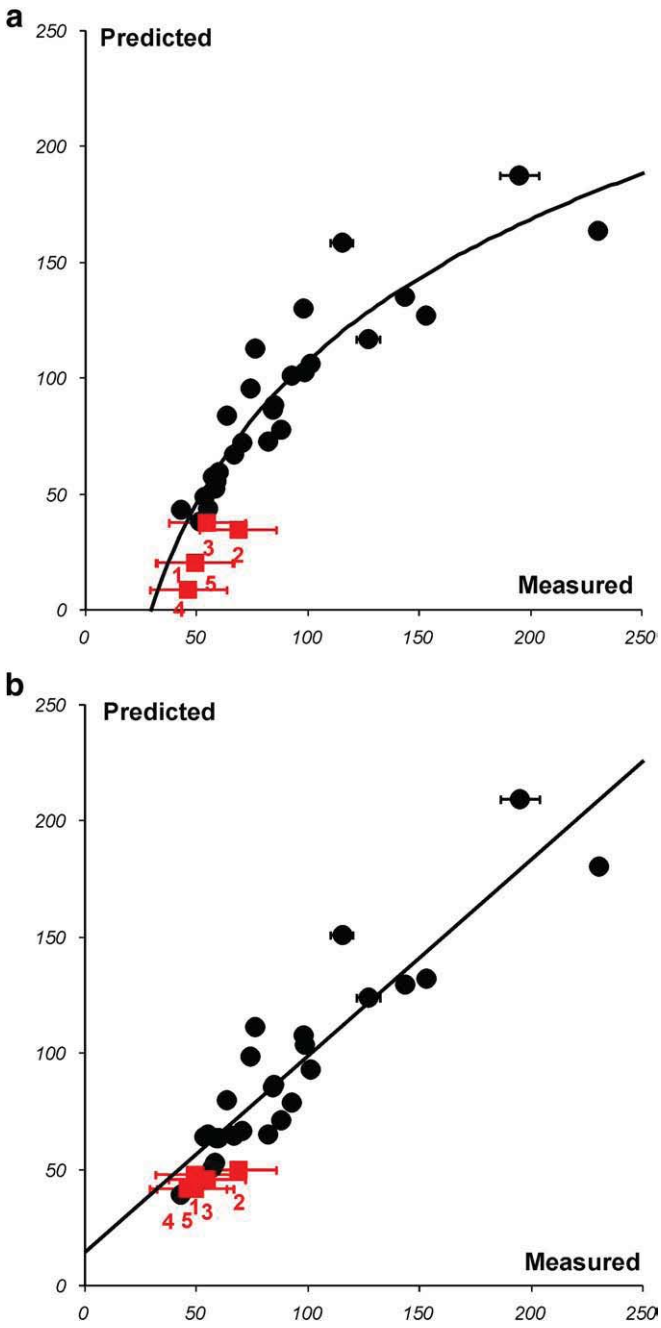

Fig. 2. Viscosity prediction. Dots are calibration values, squares with error bars are the optimized candidates. a) PCR model; b) Two-step NPCR model.

the $\mathbf{X} \rightarrow \mathbf{Y}$ regression shows a nonlinear dependence between **X** and **Y** and very poor prediction ability. See, for example, Fig. 2a that presents the PCR predicted vs. measured data for response y_2, i.e. viscosity. The similar case is observed for other properties: correlation coefficient for hardness $r^2 = 0.44$ and for compression $r^2 = 0.37$.

To account for nonlinearity we apply a two-step procedure described in the previous section. The PCA model with two PCs explains 99% of data variation in the **X** block. The scores plot for $\mathbf{t}_1$ vs. $\mathbf{t}_2$ is presented in Fig. 1b. Using $\mathbf{t}_1$ and $\mathbf{t}_2$ a new predictor (27×5) matrix **Z** is composed, $\mathbf{Z} = (\mathbf{t}_1, \mathbf{t}_2, \mathbf{t}_1\mathbf{t}_2, \mathbf{t}_1^2, \mathbf{t}_2^2)$, where all products $\mathbf{t}_a \cdot \mathbf{t}_b$ are element-wise. Afterwards **Y** is regressed upon **Z**, and each variable y_j is described by its own model (1) with the specific regression coefficients. The predicted response may be presented as a contour map, or otherwise, as a two-dimensional surface, which depends on two variables $\mathbf{t}_1$ (PC1) and $\mathbf{t}_2$ (PC2). For example, Fig. 3a presents a contour map for property y_{10} (conversion). Black dots are the **X** data projected by PCA model onto the scores plane. Colour intensity reflects the value of predicted y_{10}. Fig. 3b presents response y_{10} value as a surface over the PC1–PC2 plane.

Visual examination of all contour maps and analysis of the predicted properties (Figs. 4, 5, and similar plots for other responses)

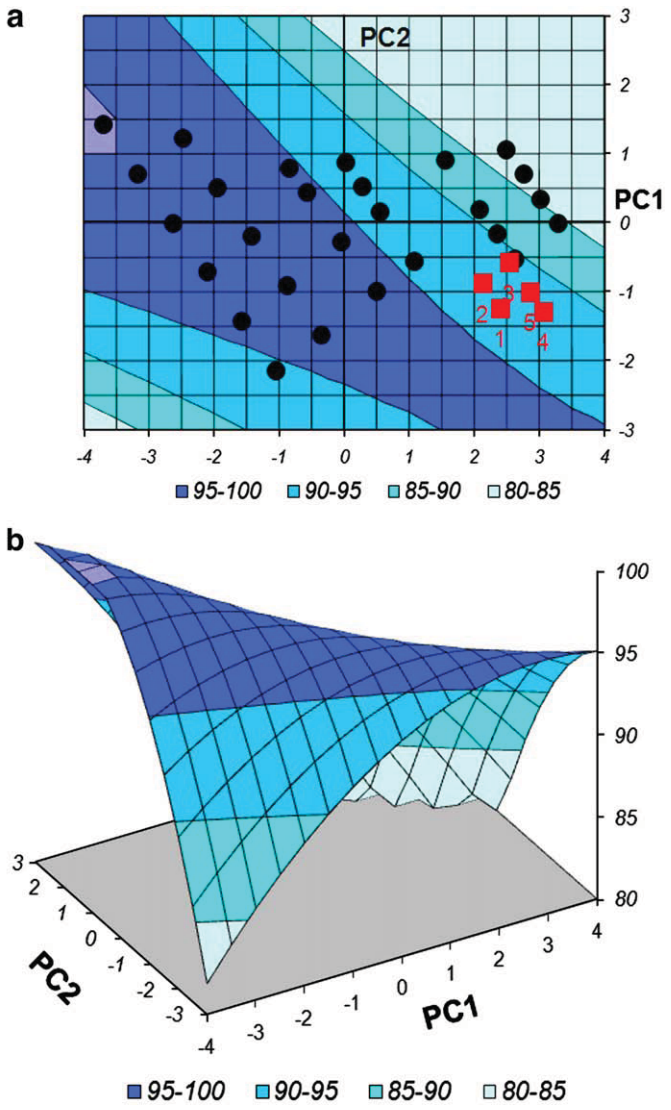

Fig. 3. Conversion level predicted by NPCR. Color intensity reflects the property value. a) Contour map. Dots are calibration points, squares are the optimized cadidates; b) 3-D surface model.

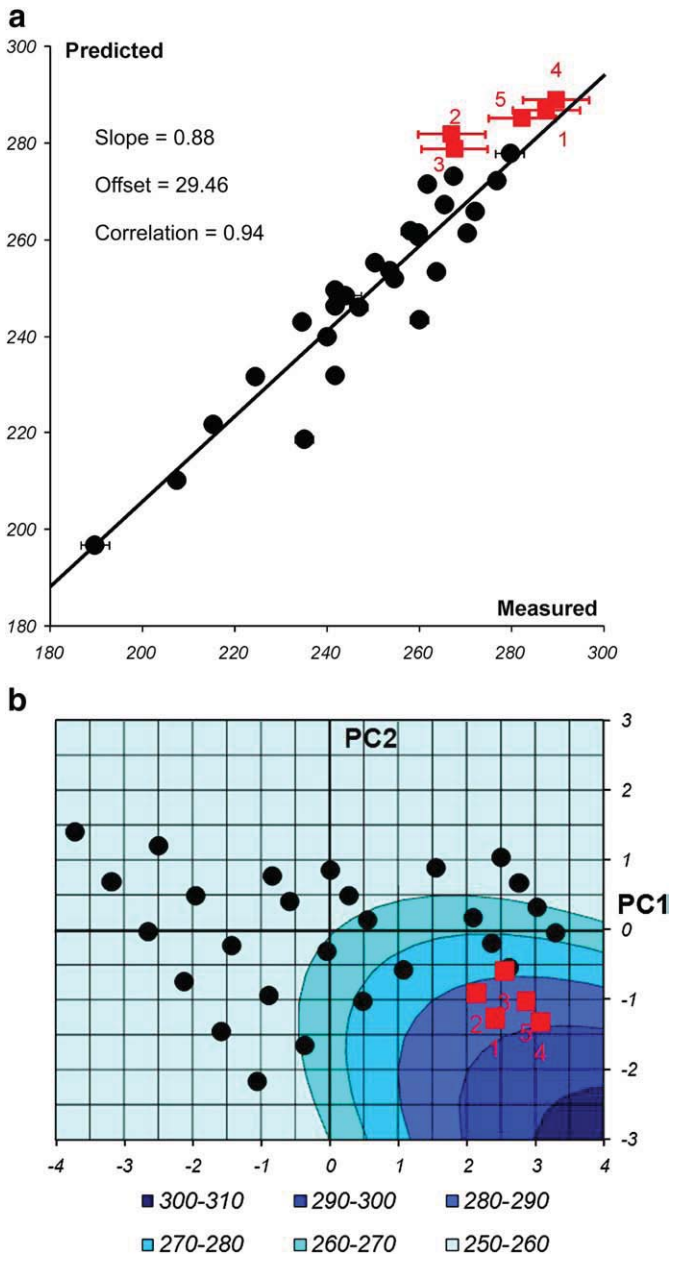

Fig. 4. Heat resistance predicted by NPCR. Dots are calibration values, squares (with error bars) are the optimized candidates. a) Predicted vs. measured plot. b) Contour map. Color intensity reflects the property value.

help us to suggest five points, $\mathbf{T}_{opt}$, which are the candidates for the optimal values (squares in all figures). These new points are located in the scores plane in the peripheral area regarding the calibration samples (Fig. 1b).

Optimized candidates $\mathbf{T}_{opt}$ are chosen with respect to the optimal binder composition requirements, which are shown in Table 1, column 2. Optimization is focused on attaining a binder with a higher heat stability, higher compression strength, higher conversion value, and lower viscosity.

3.2. Verification

To verify the proposed solution a new experiment is performed. It is aimed to confirm both the satisfactory quality of the designed binders and the prediction ability of the NPCR models (squares in Fig. 2b, 4a, 5a).

The PC values $\mathbf{T}_{opt}$ are recalculated into original $\mathbf{X}_{opt}$ values to obtain five binder formulations. It is worthy to mention that proposed

new predictor values satisfy the dependencies indicated in Fig. 1a. The organic components were synthesized and compositions were mixed, processed, tested, and corresponding $\mathbf{Y}_{test}$ values were obtained. On the other hand, the constructed NPCR models (see Eq. (1)) are utilized to predict $\mathbf{Y}_{opt}$ properties for the scores values $\mathbf{T}_{opt}$.

Measured values $\mathbf{Y}_{test}$ were compared with predicted values $\mathbf{Y}_{opt}$. Table 2 represents the relative prediction errors

$$1 - y_{test} / y_{opt}$$

calculated for each optimized mixture and for all **Y** properties. The last column of Table 2 demonstrates the reference values calculated as the ratio of the root mean square error of calibration (RMSEC) to the mean value of the corresponding response. Property y_9 (processing time) is of special kind among other **Y**-values. This is not the measured but an assigned value that defines the duration of the processing. However, it was included in the list of the responses, as

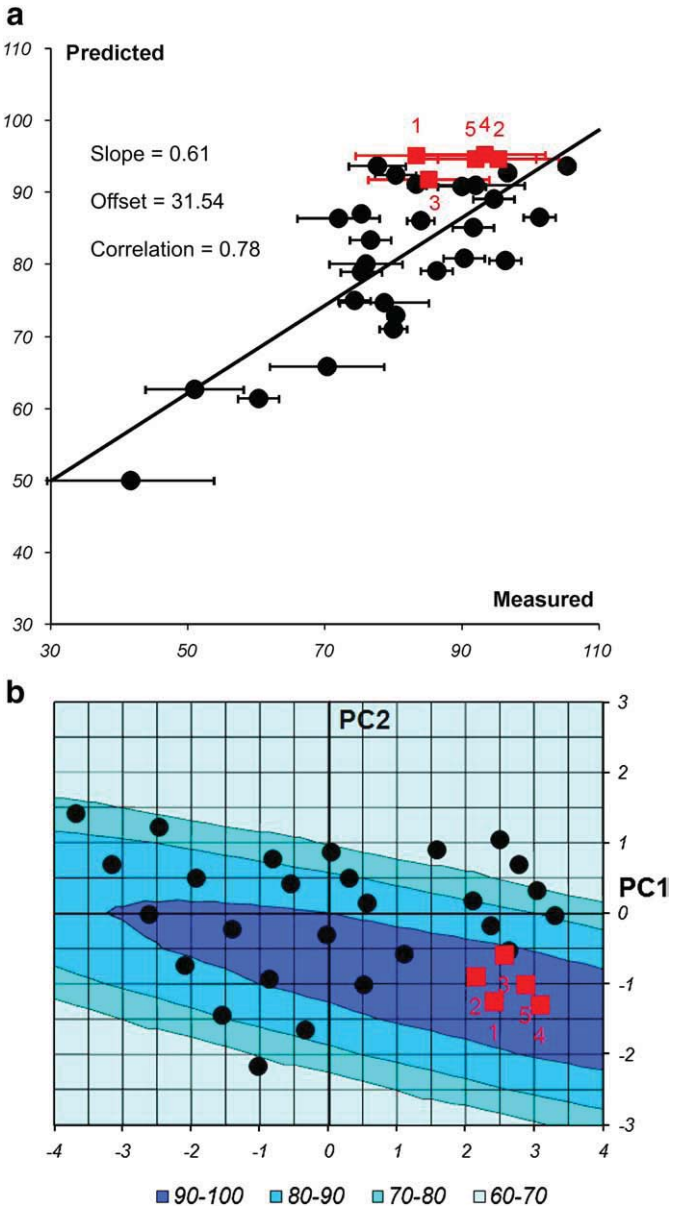

Fig. 5. Compression strength predicted by NPCR. Dots are calibration values, squares (with error bars) are the optimized candidates. a) Predicted vs. measured plot. b) Contour map. Color intensity reflects the property value.

Table 1
Requirements for the most important binder properties and their optimized values.

Property	Requirements	Sample 1		Sample 5	
		Predicted	Measured	Predicted	Measured
Thermal stability	$Y>250$	286.8 ± 8.4	287.5 ± 6.4	285.1 ± 8.4	282.3 ± 6.4
Compression strength	$Y>80$	95.1 ± 6.2	83.3 ± 3.7	94.6 ± 6.2	92.0 ± 3.7
Conversion	$Y>90$	93.5 ± 1.0	94.3 ± 1.8	91.8 ± 1.0	93.5 ± 1.8
Viscosity	$Y<130$	48.0 ± 10.2	49.0 ± 1.4	41.6 ± 10.2	49.3 ± 1.4

Table 2
Relative deviations of the predicted values from the measured properties for optimal samples (1–5) in the verification test.

Property	1	2	3	4	5	RMSEC/mean
Water resistance	−3%	−4%	3%	0%	−3%	21%
Wetting angle	−18%	5%	12%	−9%	−8%	15%
Compression strength	−14%	1%	−8%	−2%	−3%	11%
Conversion	1%	N/A	N/A	N/A	2%	2%
Elasticity	−32%	N/A	−25%	N/A	−10%	29%
Hardness	0%	−6%	−8%	−29%	−4%	9%
Thermal stability	0%	−6%	−4%	0%	−1%	3%
Gelatination time	3%	−1%	−6%	0%	0%	13%
Processing time	−1%	8%	0%	2%	1%	9%
Viscosity	2%	28%	16%	10%	16%	19%

the processing time should be adjusted together with other binder properties to obtain the better final quality.

Relying on the results of the verification test two of five proposed mixtures are selected as the optimal ones. They are No1 and No5. Their predicted and measured values together with the quality requirements are presented in Table 1. Errors' limits (±) are calculated as follows. For the measured **Y** they are the averaged standard deviations obtained from the replicated calibration data. For the predicted **Y** the errors are equal to the corresponding RMSEP value obtained with 5 test samples $\mathbf{T}_{opt}$.

4. Conclusions

The study demonstrates the benefits of chemometric approach in application to engineering. The nonlinear PCR solves a complex nonlinear multivariate optimization problem employing a simple projection approach and graphical representation of the models. The input variables' reduction gives an opportunity to choose the optimal binder formulations visually without complicated numerical procedures. The suggested optimal formulations have been verified by the additional experiment. The test confirmed that optimized binders meet the predefined quality requirements. Two formulations are recommended to employ in the routine production of the composite materials.

The distinctive feature of the proposed binders is the absence of diluents. This makes the materials safer both in production and in application. The composites usability has been confirmed by practical implementation [21]. The developed binders have been used in production of the foamed polyurethane and the basalt-plastic reinforcements. It has been shown that both materials exceed analogues in thermo- and heat-resistance.

References

[1] F. Yacoub, J.F. MacGregor, Chemom. Intell. Lab. Syst. 70 (2004) 63–74.
[2] K. Muteki, J.F. MacGregor, T. Ueda, Ind. Eng. Chem. Res. 45 (2006) 4653–4660.
[3] A.L. Pomerantsev, O.Ye. Rodionova, A. Höskuldsson, Chemom. Intell. Lab. Syst. 81 (2006) 165–179.
[4] A. Höskuldsson, O.Ye. Rodionova, A.L. Pomerantsev, Chemom. Intell. Lab. Syst. 88 (2007) 84–99.
[5] S. Wold, N. Kettaneh-Wold, B. Skagerberg, Chemom. Intell. Lab. Syst. 7 (1989) 53–65.
[6] V. Taavitsainen, P. Korhonen, Chemom. Intell. Lab. Syst. 14 (1992) 185–194.

[7] W. William Hsieh, Neural Netw. 20 (2007) 434–443.
[8] P.C. Hewlett, Lea's Chemistry of Cement and Concrete, Fourth EditionButterworth Heinemann, 2003.
[9] Silicon-based material and devices, in: Hari Nalwa (Ed.), Hardbound, Academic Press, 2001.
[10] H. Chujo, T. Saegusa, Organic polymer hybrids with silica gel formed by means of sol–gel method, Adv. Polym. Sci. 100 (1992) 11–29.
[11] S.S. Ivanchev, A.M. Mesh, N. Reichelt, S.Ya. Khaikin, A. Hesse, S.V. Myakin, Preparation of nanocomposites by alkoxysilane hydrolysis in a polypropylene matrix, Polym. Sci. A 44 (2002) 623–626.
[12] S. Wang, Z. Ahmad, J.E. Mark, Polyimide-silica hybrid materials modified by incorporation of organically substituted alkoxysilane, Chem. Mater. 6 (1994) 943–946.
[13] Z. Ahmad, J.E. Mark, Polyimide-ceramic hybrid composites by the sol–gel route, Chem. Mater. 13 (2001) 3320–3330.
[14] S. Chen, J. Sui, L. Chen, Positional assembly of hybrid polyurethane nanocomposites via incorporation of inorganic building blocks into organic polymer, Colloid Polym. Sci. 283 (2004) 66–73.
[15] Ye.P. Mamunya, V.I. Shtompel, E.V. Lebedev, P. Pissis, Structure and water sorption of polyurethane nanocomposites based on organic and inorganic components, Eur. Polym. J. 40 (2004) 2323–2331.
[16] S. Grishchuk, N. Castella, J. Karger-Kocsis, Hybrid resins from polyisocyanate–vinyl ester–water glass system: structure and properties, Eur. Polym. J. 43 (2007) 2323–2331.
[17] E.V. Lebedev, S.S. Ishchenko, V.D. Denisenko, V.O. Dupanov, E.G. Privalko, A.A. Usenko, V.P. Privalko, Effect of organic modifying agents on formation of organosilicate polymeric formulations, Russ. J. Appl. Chem. 71 (1998) 2055–2058.
[18] S.S. Ishchenko, A.B. Pridatko, T.I. Novikova, E.V. Lebedev, Interaction of isocyanates with aqueous solutions of alkali metal silicates, Polym. Sci. A 38 (1996) 485–490.
[19] V.I. Pavlov, S.S. Ischenko, E.I. Fedorchenko, Strength properties of some organosilicate polymeric compositions, Plast. Massy (6) (1996) 36–38 (in Russian).
[20] L.A. Abdarakhmanova, I.A. Starovoitova, V.G. Khozin, Prospects of application of organo-mineral binders in building materials, Build. Mater. (9) (2007) 2–4 (in Russian).
[21] I.A. Starovoitova, Izv. KGASU (2) (2007) 89–94 (in Russian).